Ductile-Fracture Resistance in X100 Pipeline Welds Measured with CTOA

Use of the crack tip opening angle test for determining resistance to ductile fracture of high-strength welded pipeline materials was evaluated

BY E. DREXLER, P. DARCIS, C. N. McCOWAN, J. W. SOWARDS, D. McCOLSKEY, AND T. A. SIEWERT

ABSTRACT

A test for evaluation of resistance to ductile fracture [crack tip opening angle (CTOA)] was found to reveal changes in crack extension through the heat-affected zone (HAZ) and weld interface in X100 pipeline steels. This test provides a long ligament for crack extension data not available in Charpy or drop-weight tear specimens, and is much less expensive than the full-scale burst tests. The ductile-fracture resistance of girth welds, perpendicular to the growing crack, and seam welds and their HAZs, parallel with the crack, were evaluated. Analysis of the data reveals some general differences, such as changes in CTOA and crack extension rate as the crack moved through the base metal, HAZ, and girth weld material. The values for CTOA were observed to increase and the crack extension rate decreased as the crack moved through the weld and approached the weld interface. The plastic deformation appears to be strongly influenced by the properties and geometry of the narrow HAZ, the weld interface, and the tougher base material. Consequently, the CTOA of the HAZ associated with the girth weld was larger than that of the seam-weld HAZ. It was not possible to obtain CTOA data for the seam weld with the crack parallel within the weld, because the crack immediately diverted out of the weld material into the HAZ. The CTOA values from both girth welds and seam-weld HAZ were smaller than those of the base material.

Introduction

Crack tip opening angle (CTOA) is a crack ductility test that is widely accepted for assessing the likelihood of steady-state tearing behavior in the aluminum alloys found in older aircraft. Recently, it has gained acceptance in the pipeline community as a fracture parameter for pipeline design (Refs. 1, 2). The modified double cantilever beam (MDCB) specimen design advocated by Hashemi et al. (Refs. 3, 4) and Shterenlikht et al. (Ref. 5) was adopted for this work. Advantages of this specimen design include a long ligament arm (200 mm) for steady-state tearing and higher constraints, approaching those seen in pipeline material in service (Ref. 4). This design has been used successfully to generate values for the resistance to crack extension for pipeline base metals, such as X52, X80, and X100 (Refs. 6, 5, 3, respectively).

Welding of X100 base metal has many simultaneous challenges. Beyond the difficulty of obtaining a weld that is compatible with the base material under static loads, there are the complexities of understanding the influence of the weld should a running crack initiate and then propagate due to the combination of loads from service pressure, other factors such as third-party damage and any ground movement, and residual stresses introduced during the joining process (Refs. 7, 8).

KEYWORDS

Crack Extension
Crack Tip Opening Angle (CTOA)
Ductile Fracture
Ductile Tearing
Heat-Affected Zone (HAZ)
Submerged Arc Welding (SAW)
Shielded Metal Arc Welding (SMAW)
Stable Tearing
Welds

E. DREXLER (Drexler@boulder.nist.gov), *P. DARCIS, C. N. McCOWAN, J. W. SOWARDS, D. McCOLSKEY, and T. A. SIEWERT are with National Institute of Standards and Technology (NIST), Boulder, Colo.*

Contribution of the National Institute of Standards and Technology, an agency of the U.S. government; not subject to copyright in the U.S.A.

Crack tip opening angle measurements can provide this more global structural perspective by indicating whether the joints in the fabricated structure have the same resistance to crack extension as is seen with the fairly uniform base metal. Seam welds, girth welds, and their associated heat-affected zones (HAZs) are each of concern, separately and in concert.

Tests of the various regions within the pipe (like tensile or Charpy impact tests of the base material, HAZ, and weld) are needed to confirm that each region satisfies the design minimums, but they cannot adequately measure the composite behavior of these regions in the fabricated pipe.

This work evaluates the usefulness of CTOA measurements made with MDCB specimens in the complex and composite structure of a weldment, as it quantifies the resistance to crack extension for each of the weld regions. Crack tip opening angle testing of the MDCB specimen has several benefits (Refs. 6, 9). It permits multiple measurements of the CTOA from a single specimen (perhaps as many as 50 or 60 over a 40-mm distance). This allows measurement of the behavior as the crack enters and leaves the girth weld region that encompasses the base material, HAZ, and weld metal. Another benefit of using the MDCB specimen is that the test section does not restrain the transition to slant mode shear fracture.

Procedure

Materials

Weld material and the associated HAZ from X100 experimental pipelines were tested with MDCB specimens to obtain CTOA data. The certified composition for X100 pipeline is found in Table 1. The sections had a diameter of 1.32 m (52 in.) and were 20.6 mm (0.81 in.) thick. The pipe was received already welded. Girth welds were made manually with shielded metal arc welding (SMAW), and seam welds were produced by automatic submerged arc welding (SAW) with materials and procedures representative of future field production. More details on the se-

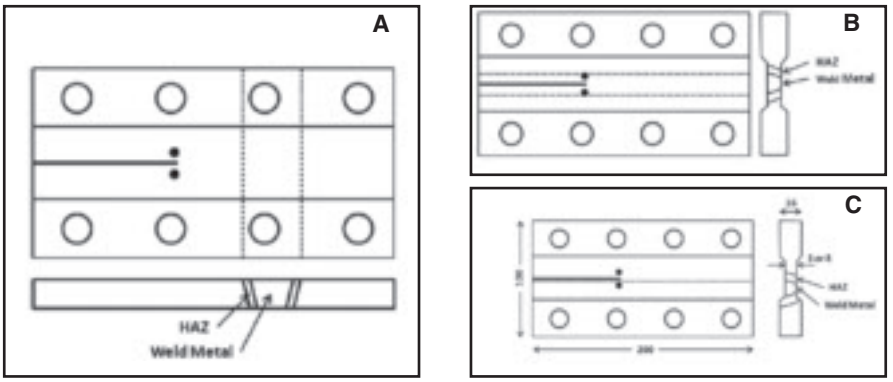

Fig. 1 — MDCB specimen configurations for evaluation of CTOA: A — Crack growth transverse to the girth weld; B — crack growth in weld metal of the seam weld; C — crack growth in the HAZ of the seam weld. Nominal specimen dimensions (mm) are shown in C.

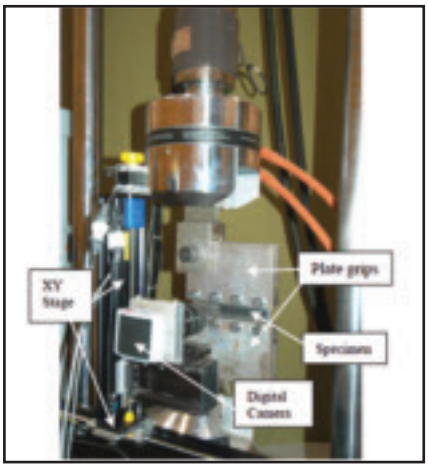

Fig. 2 — CTOA test setup.

Table 1—Certified chemistry of X100 Base Material

Al	C	Cr	Cu	Fe	Mn	Mo	N	Nb	Ni	P	S	Si	Ti	V
0.025	0.084	0.021	0.286	Balance	2.092	0.127	0.005	0.041	0.501	0.010	0.002	0.108	0.007	0.006

Table 2 — Tensile Properties of X100

Orientation	$\sigma_{0.2}$ (MPa)	σ_{UTS} (MPa)	$\sigma_{0.2}/\sigma_{UTS}$	e_u (%)	e_f (%)	e_u/e_f
Base Metal (Trans.)	798	827	0.97	4.1	19.3	0.21
Base Metal (Long.)	732	806	0.91	4.6	20.3	0.23
Girth Weld (Trans.)	730	835	0.87	7.7	15.0	0.51
Seam Weld HAZ	642	693	0.93	4.1	12.1	0.34

quences are included in the section on microstructural characterization. However, details of the weld procedure are unknown. The tensile properties of the base metal, girth weld, and seam weld HAZ are shown in Table 2. Round tensile specimens were machined from desired locations of the pipe material and tested according to ASTM E8 standard test method for tension testing. Girth weld specimens were taken transverse to the axis of the pipe and were all weld metal in the gauge section.

Flat MDCB specimens were ground from the curved pipe. This approach avoids mechanical flattening, which introduces plastic deformation in the specimens. Figure 1 shows the specimen dimensions and the positioning of the weld location with respect to the notch for the various tests. The specimens were machined with the notch aligned with the axis of the pipe, the expected direction of a running crack. An initial straight notch (1.6 mm width × 60 mm length) was machined through the specimen thickness as indicated. The notch length was measured from the load-line of the pins in the test fixture. The fixture is shown in Fig. 2 and discussed below. A laser was used to scribe a 1 mm × 1 mm, or 1 mm × 0.5 mm, grid on the test section to aid in the CTOA measurements with the use of image analysis software.

CTOA Testing

Detailed CTOA test procedures can be found in the literature (Refs. 6, 9), but are described here briefly. Figure 2 shows the test setup, which utilized optical imaging (a digital charge-coupled device camera) to record images of the crack tip for post-test analysis of the CTOA of each material studied. The loading of the specimen was facilitated through the use of a pair of thick plate grips bolted to the side surfaces of the specimen — Fig. 2. Two cylindrical pins provided free rotation of the whole assembly (specimen plus loading plates) during the experiments. Tightly clamping the grip section with the two thick loading plates increased the constraint levels in the gauge section. The long uncracked ligament and the loading geometry provided a condition that allows stable crack extension in the specimen ligament similar to that of crack extension in a real structure (Ref. 4). The load-line was between the left pair of holes where the grips were bolted.

The test matrix is shown in Table 3. A servo-hydraulic testing machine with a load capacity of 250 kN (55 kip) was used to initiate a fatigue crack at the 60-mm-long chevron notch and extend it an additional 5 to 10 mm. The subsequent CTOA tests were run in displacement mode at a crosshead velocity of 0.002 mm/s for one girth weld specimen of each thickness, and 0.02 mm/s for the remaining specimens.

The effect of specimen thickness on CTOA was investigated by testing two different thicknesses, either 3 or 8 mm thick. Additionally, specimens were produced from three different locations on the linepipe. One location tested the girth weld, a second the seam weld, and the third the HAZ associated with the seam weld. With the specimen configuration used, data on ductile-fracture resistance were generated as cracks ran perpendicularly to girth welds, and parallel with the seam welds and their associated HAZ, which were centered in the test section of those specimens. The test sections were acid etched and neutralized to make the weld and HAZ visible.

CTOA Measurement

Analysis of the images was conducted with commercially available image-analysis software, augmented with customized macros. The collected images were screened to meet minimum standards, such as having adequate focus and 1 mm of straight crack extension beyond the initial crack blunting. Crack extension in weld material was generally more erratic than in base metal. The analysis was also modified slightly from that reported in Darcis et al. (Refs. 6, 9). For the data reported here, the crack edge was traced by an operator for a distance of approximately 2 mm back from the crack tip to capture the data associated with the crack.

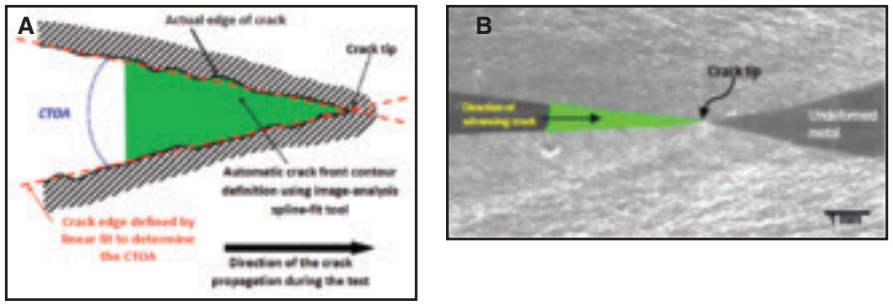

Fig. 3 — A — Graphical representation of how the CTOA values are determined; B — an example of a crack opening (CTOA = 10 deg) highlighted in green. The crack is advancing from the left. The undeformed region of the specimen is seen as the dark triangle to the right at the tip of the crack.

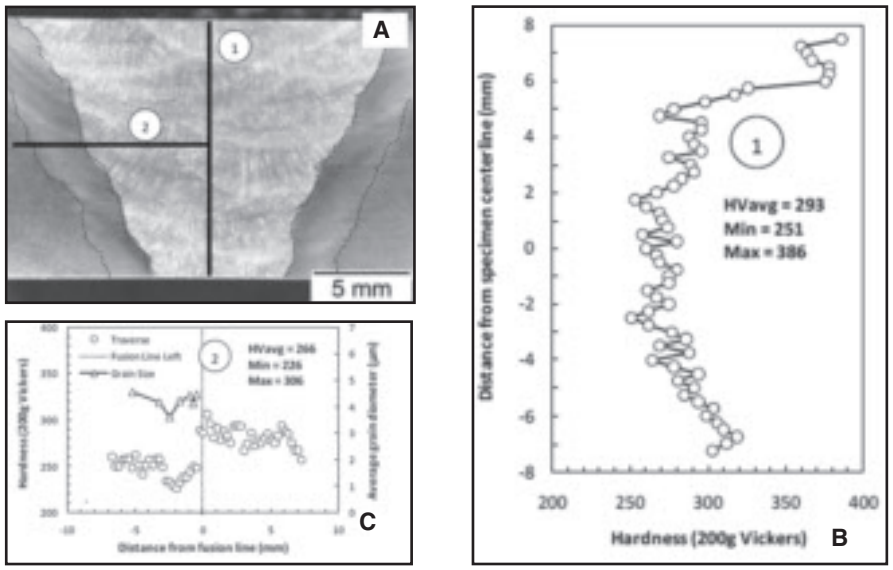

Fig. 4 — A— Girth weld cross section indicating regions where hardness traverses were measured; B — the corresponding microhardness traverse results; C — the grain size results.

Intersecting lines were then fit to 100 points of the upper and lower flank of the crack edge and the CTOA was calculated from the angle formed by the intersection of those fits — Fig. 3A. For each analyzed image, the CTOA value and the crack length were recorded. Figure 3B shows a crack opening highlighted in green, advancing from the left in a HAZ region. The area is highly deformed above and below the crack opening, but deformation extends only a short distance directly ahead of the crack tip. The undeformed region is seen as the dark area to the right of the crack tip, mirroring the triangular shape of the open crack.

Metallography

Metallographic samples were sectioned from the CTOA test specimens to determine microstructure and hardness of the weld regions. Samples were mounted, ground, polished to a 1-μm finish, and etched in 2% nital. Metallography was performed on the etched specimens with light optical microscopy. Grain-size measurements were performed with commercially available image-analysis software designed for microscopy applications. Grain areas were measured and equivalent grain diameters were determined with the assumption of a spherical grain. Some metallographic mounts were also subjected to Vickers hardness testing. A load of 200 g was used for the indentations and an indent spacing of 250 μm was typically used for hardness traverses across the weld regions. Fracture samples were also sectioned from the fractured weld regions and cleaned ultrasonically in methanol. Scanning electron microscopy (SEM) was performed on the fracture surfaces with an accelerating voltage of 10 kV.

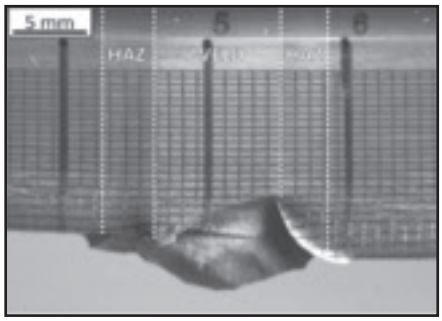

Fig. 5 — An example of the fracture through a girth weld. The approximate locations of the weld interfaces and edge of the HAZ are indicated. The crack jumped through the first HAZ to the left.

Microstructural Characterization

Microstructures of the girth and seam welds directly from CTOA specimens were evaluated to relate the metallurgical structure of the welds to the fracture behavior observed during the CTOA testing. Results of this evaluation, including micrographs, hardness traverses, and grain-size measurements are presented below.

Girth Weld

Figure 4A shows the etched cross section of the girth weld from a CTOA specimen, that is, perpendicular to the testing direction. Note the V-groove deposit consists of multiple passes. The weld deposit was approximately 8 mm in width at the bottom. This width corresponds to the specimen face and fracture shown in Fig. 5. The boundaries of the HAZ associated with the girth weld have been highlighted in Fig. 4A and were determined to be between 2 and 3 mm in width.

Vickers hardness traverses were performed vertically at the weld centerline

Table 3 — Test Matrix

Condition/Specimen Type	Girth Weld	Seam Weld	Seam Weld HAZ	Base Metal
3 mm, displacement rate = 0.02 mm/s	1	2	2	2
3 mm, displacement rate = 0.002 mm/s	1	0	0	0
8 mm, displacement rate = 0.02 mm/s	2	2	2	3
8 mm displacement rate = 0.002 mm/s	1	0	0	0

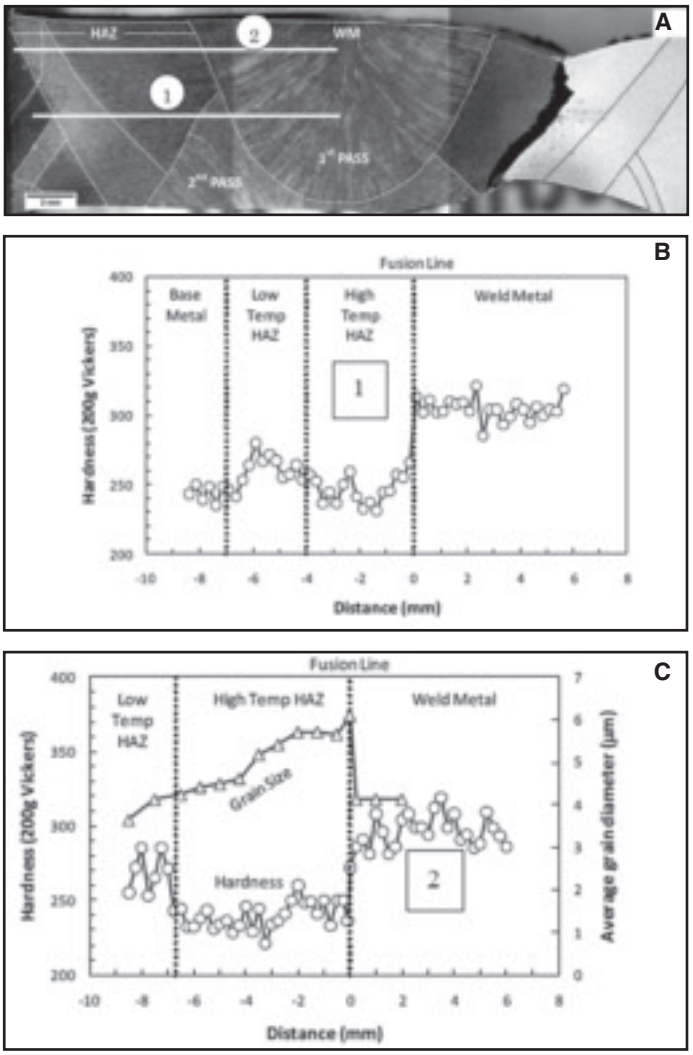

Fig. 6 — A — Cross section of seam weld CTOA specimen indicating fracture location; B, C — corresponding microhardness; C — corresponding grain size measurements at locations indicated.

and horizontally across this cross section. The resulting hardness profiles of the vertical and horizontal traverses are shown in Fig. 4B and C, respectively. The hardness traverse in Fig. 4B shows that the reheating due to additional weld passes resulted in hardness variations through the thickness. The reduced sections of the MDCB specimens were machined so that the specimen thickness corresponded to the area between –4 and 4 mm of this traverse. Therefore, the CTOA test specimens likely had minimal variability in hardness, with average hardness of approximately 270 Vickers hardness number (HV). The horizontal hardness traverse in Fig. 4C shows that the base-metal hardness was on the order of 250 HV. Hardness decreased as the traverse entered the HAZ from the base metal, by approximately 10%. However, hardness recovered somewhat as the traverse approached the weld interface. Peak hardness values were achieved in the weld metal, where measured values were on the order of 300 HV. This increase in hardness was a result of overmatched weld deposits.

The average grain size from the base metal to the weld interface is also shown in Fig. 4C. The grain size varied between about 4.5 μm in the base metal to about 3.75 μm in one location in the HAZ. Note that the decrease in grain size was in the same region where a drop in hardness was observed. Possible explanations for this softening could be transformation to a softer bainitic structure than the base metal upon cooling, or perhaps recrystallization or recovery; however, such an observation was not possible in the current work due to the limitations of light optical microscopy.

Seam Weld

The features of the seam weld were very different from those of the girth weld. Figure 6A shows a cross section of the entire weld after CTOA testing. The weld was accomplished in two passes, the first side and the second side, and both have a distinctive columnar grain structure. The weld itself is approximately 13 mm across at the first side and 14.5 mm at the second side, and the HAZ can be seen 8 mm beyond the weld interface. Four distinct HAZ regions were visible, two associated with the first pass, and two associated with the second pass. The two regions associated with each pass will be referred to as the high-temperature, adjacent to the weld, and the low-temperature HAZs.

Each region had different hardness and average grain sizes, as seen in Fig. 6B, C. The hardness levels of the base metal, the low-temperature HAZ, the high-temperature HAZ, and the weld metal were approximately 250, 275, 250, and 300 HV, respectively. Grain sizes varied substantially between the base metal [3.5 μm, Fig. 7A] and the HAZ adjacent to the weld interface [5.7 μm, Fig. 7B]. Note that grain coarsening apparently did little to affect the hardness in the corresponding regions. Although a decrease in hardness (proportional to strength) may be expected with an increase in grain size, the transformation of the coarsened prior-austenite grains in the high-temperature HAZ to harder constituents (such as martensite or

Table 4 — Data on the Mean Value of CTOA from Each Specimen and for All Specimens for the Given Thickness

	Girth Weld				Seam Weld HAZ		SeamWeld→HAZ		Base Metal	
	HAZ[a]		Weld							
	Mean (°)	SD[b] (°)	Mean (°)	SD (°)	Mean (°)	SD (°)	Mean (°)	SD (°)	Mean (°)	SD (°)
3 mm: all	10.6	1.7	3.0	1.1	4.0	1.1	3.8	1.6	4.2	0.8
1	10.7	1.1	2.7	0.8	4.2	1.3	4.9	1.6	4.3	0.9
2	9.9	2.8	4.9	NA	3.8	0.9	3.0	1.1	4.1	0.8
8 mm: all	10.7	2.6	6.8	1.7	7.0	1.3	6.1	1.4	8.7	2.0
3	8.3	2.4	5.5	1.4	7.2	1.3	6.5	1.2	8.5	1.0
4	13.1	1.1	7.6	1.5	6.5	1.1	5.7	1.5	8.4	2.6
5	11.2	1.9	7.4	1.6					9.0	2.2

(a) HAZ here refers to the observed composite behavior of the joint.
(b) SD = standard deviation.

bainitic ferrite constituents) likely increased hardness to counteract the drop in hardness from increasing grain size. Larger (~ 50 μm) prior-austenite grains are evident near the fusion boundary — Fig. 7B.

CTOA Test Results

Base Metal

Before describing the behavior of the weld tests, it is useful to discuss the behavior of the base metal alone. Figure 8 shows the typical plot of force vs. crosshead dissplacement for a CTOA test of X100 pipeline material that was 8 mm thick in the gauge section and tested at 0.02 mm/s. Characteristic crack features associated with different junctures in the load-displacement sequence are also indicated. Note that the applied load increased linearly while the specimen remained in the elastic regime. At the onset of plastic deformation, the loading rate, proportional to the slope of the curve, continually decreased as plastic strains increased. A crack began to develop near the peak load, although some additional displacement was required for it to propagate in the sharp manner shown in Fig. 3. A well-developed crack was observed near the peak load and began to advance with displacement, with the overall applied load decreasing in proportion to the remaining cross-sectional area of the specimen. That is, as the crack advanced, the load necessary to cause crack extension decreased, typical of plastic collapse.

Girth Weld

Five girth weld specimens were tested with the crack oriented transverse to the weld, so that the path of the growing crack would pass through base metal, HAZ, weld interface, weld metal, weld interface, HAZ, and base metal. Two specimens were machined to a thickness of 3 mm; three specimens were machined to a thickness of 8 mm. One specimen of each thickness was tested at a crosshead velocity of 0.002 mm/s, while the remaining specimens were tested at 0.02 mm/s. Since the crack ran perpendicularly to the weld, it was expected that CTOA data would be obtained on the HAZ at two locations on each specimen. However, the crack propagated so quickly through the first HAZ into the weld material that no images were captured in any of the tests conducted at 0.02 mm/s. Figure 5 depicts one of these specimens. The weld and HAZ are visible on the face of the specimen as indicated on the figure. A prominent shear lip is also present on the weld fracture surface.

Figure 9 shows the characteristic curve of force vs. displacement for CTOA tests of both uniform base metal and a specimen containing a girth weld, where the girth weld is reached at crosshead displacements between about 24 and 28 mm. Both specimens were tested at a crosshead displacement rate of 0.02 mm/s and were 8 mm thick in the gauge section. With the uniform base metal, as the loading increased, the tip of the fatigue precrack blunted. Once tearing began, the load dropped linearly with the crosshead displacement during steady-state tearing.

This behavior changed with the presence of a girth weld, however. The typical load drop associated with tearing (as observed in the base metal) was interrupted as the crack approached and entered the weld, indicated by the dashed line. It is observed that the effects of the weld on the slope of the force-displacement data are manifested well before the crack reaches the weld metal. Since the test was conducted in displacement control, crosshead displacement is directly proportional to time; therefore, a larger negative slope corresponds to greater crack-growth velocity. The data show, therefore, that the crack began growing more rapidly before entering the weld and slows before exiting the weld. Although changes in crack growth rate are not classical behavior and locally other mechanisms may dominate, the overall failure mechanism in the girth weld specimens was plastic collapse.

Corresponding to the changes in the force record, there were changes in value of the CTOA measured on the specimen as the crack propagated through the weld region. Values for the CTOA with respect to crack length for a specimen containing a girth weld, and for uniform base metal for the purpose of comparison, are shown in Fig. 10. In typical tests of the uniform base metal, high initial CTOA values drop to a fairly consistent CTOA value observed during steady-state tearing. The high initial CTOA values are due to blunting of the fatigue precrack, and steady-state tearing usually occurs when the crack length is ~2× the thickness of the specimen. The average value of CTOA from the region of steady-state tearing of the particular test shown from X100 pipeline material was ~9 deg.

Girth-weld specimens do not follow this model, however, which may be due to several factors, including the complexity

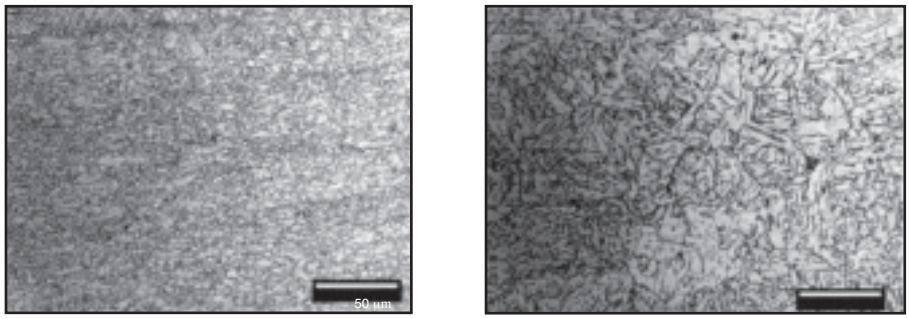

Fig. 7 — Representative images of the grain size in the base metal (left image) and adjacent to the weld interface in the high-temperature HAZ (right image).

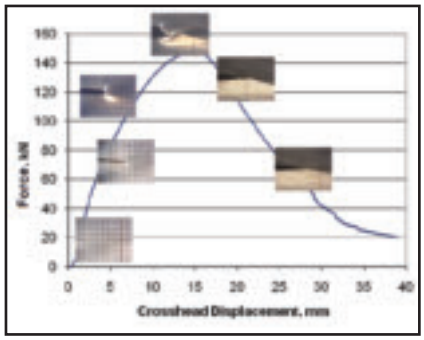

Fig. 8 — X100 test of base metal showing the characteristic crack features associated with different junctures in the force-displacement sequence.

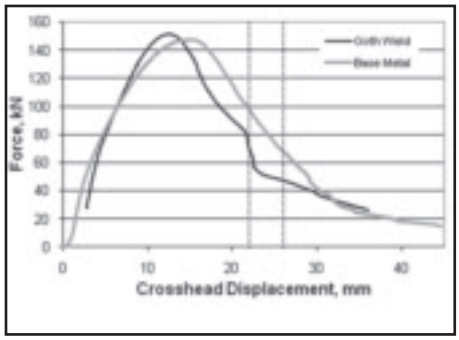

Fig. 9 — Graph showing the data of force vs. displacement for an X100 base metal and girth weld specimen. The dashed lines indicate where the crack entered and left the weld.

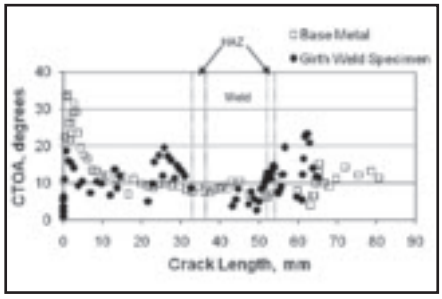

Fig. 10 — Changes in CTOA as the crack proceeds across the base metal, HAZ, and girth weld of the specimen. CTOA is shown for base metal to contrast differences in observed behavior. Specimens are 8 mm thick.

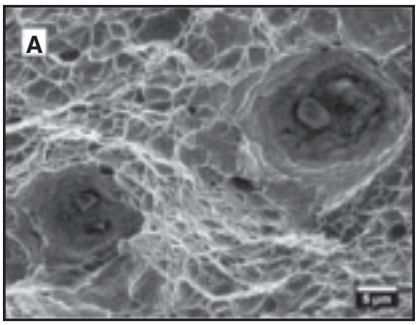

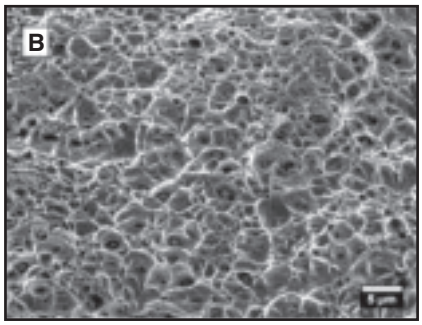

Fig. 11 — Representative images from the fracture surface: A — HAZ; B — weld metal.

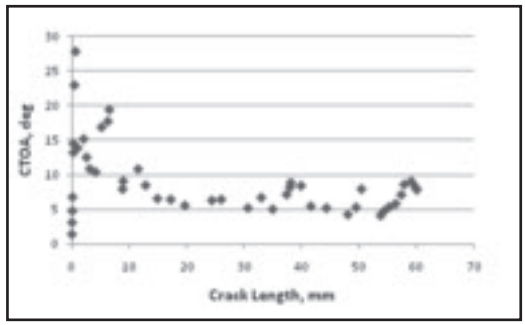

Fig. 12 — CTOA vs. crack length for a test conducted in the HAZ of a seam weld.

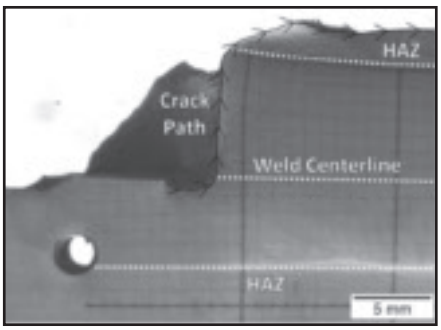

Fig. 13 — Image showing how the crack deviated from the seam weld into the HAZ.

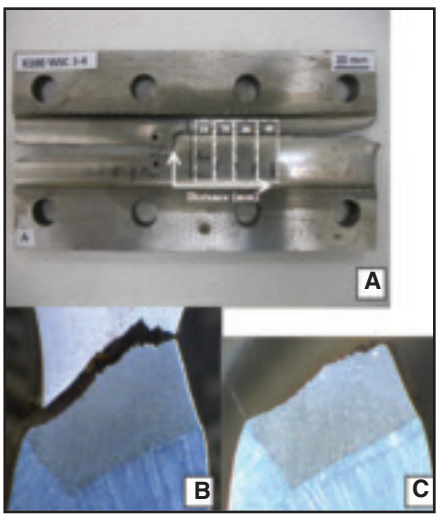

Fig. 14 — Post-test image of a seam-weld test specimen: A — Cross section of the crack in the high-temperature HAZ; B, C — 10 and 40 mm, respectively, from the end of the fatigue precrack.

of the the weld being at an angle to the approching crack front. Figure 10 shows the location of the HAZ and weld. It can be seen that once the CTOA makes its initial drop to steady-state tearing, the highest values of the CTOA appear to have no association with the HAZ, weld interfaces, or weld, but rather are found in the base metal before and after the weld. A study of the fracture surface reveals that in both instances, the fracture orientation is changing from slant to flat. It should be noted that the transition from one orientation to another results in far subtler changes in the value of CTOA in a uniform base metal specimen. An example of this is shown in Fig. 10 at about 65 mm of crack length. The influence of the weld must not be discounted, however, even though this blunting of the CTOA occurs in the base metal, as this symmetric rise in the value of CTOA is typical of the girth weld specimens, although the exact mechanisms that cause a change in the fracture orientation are not clear. The test from which the data shown in Fig. 10 were extracted had other interesting behaviors that are worth mentioning. As the crack front approached the first HAZ, a crack began opening up in the weld metal. Although these cracks were not immediately connected on the observed surface, they apparently were beneath the surface. This highlights a limitation of the CTOA test; since the measurement takes place on the surface, influences through the depth may affect surface measurements. The two cracks connected abruptly, which accounts for the gap in the CTOA data between about 33 and 43 mm. Also, as the crack was exiting the weld the crack tip blunted (larger CTOA values) at the weld interface and again at the interface between the HAZ and the base metal.

Comparisons between the fracture surface from the HAZ and weld metal of the girth weld are shown in Fig. 11A and B, respectively. Inclusions in the HAZ had a Ca-Al-Fe chemistry and the observed inclusion diameters were as large as 5 μm. Within the weld metal the inclusions were smaller, averaging just under 0.5 μm. The inclusions in the weld metal had a chemistry that included Fe-Mn-Si-Ti. Both regions showed ductile dimpling, although the dimple size was larger in the HAZ and exhibited a slight directionality, indicating a shear component to the fracture. Dimple directionality was associated with macroscopic shear fracture faces of the girth weld specimens, especially in the vicinity of the HAZ. Shear dimples were observed in base metal as well, albeit to a lesser extent. Base metal fracture surfaces were slant or double-slant, and typically changed to full slant fractures in the vicinity of the girth welds. Since shear dimples were observed at random on all fractured regions of the weldment (base metal, HAZ, and fusion zone), it is not possible at this time to relate microscopic shear features to determined values of CTOA. However, equivalent dimple diameters were smallest in the fusion zone, where the lower values of CTOA were observed and largest in the HAZ where higher values of CTOA were observed. Dimple distribution is related to the inclusion size and distribution, which in turn could be affected in the HAZ by local thermal history due to multipass welding, and thermal history and alloying in the weld metal. A relationship between dimple diameter and CTOA is unsubstantiated by this work and requires further investigation.

Several notable results were obtained during CTOA testing of the girth weld specimens. These results are as follows:

- The presence of the weld led to inconsistent behavior of the tearing crack, as the crack jumped through the first HAZ, joining with an already-initiated crack in the weld, and the second HAZ generated a larger CTOA than the weld.
- The CTOA of the weld material was significantly smaller in the 3-mm specimens, as compared with the 8-mm specimens. This finding was determined to be statistically significant based on the use of a student's T-test, where $p < 0.0001$. Table 4 shows the mean and standard deviation of each specimen tested and for all specimens for the given thickness.
- In every case, as the crack approached the weld interface when exiting the weld, the crack extension slowed or stopped as the crack tip blunted. This blunting resulted in an increase in the CTOA. This increase was as little as 59% higher than the mean value for the CTOA within the weld, to as much as 213% higher. The increase in CTOA was also associated with a plateau or abrupt decrease in slope in the load-displacement curve for the test.
- The loading displacement rate appeared to have had a small effect on the CTOA values. In the two slower tests con-

ducted on girth welds, the CTOA values were smaller than the mean of the tests conducted at 0.02 mm/s. However, measured values of CTOA at the slower rates were still within one standard deviation. This agrees with observations of Reuven et al. (Ref. 10), where the authors found that neither crosshead displacement rate nor crack velocity had a significant effect on CTOA values of X100 pipeline base metal.

Seam Weld

Four specimens, two of each thickness, were tested at a crosshead displacement rate of 0.02 mm/s with the HAZ from a seam weld centered in the test section. As with the girth welds, significant differences in the CTOA ($p<0.0001$) were found depending on the thickness of the test section (see Table 4). Figure 12 is an example of a CTOA test conducted with the crack growing in the HAZ of a seam weld. This material behaves similarly when compared to that of the base metal in Fig. 10, although values for CTOA in the steady-state region are generally lower.

Four seam weld specimens were tested in two thicknesses at a displacement rate of 0.02 mm/s. The specimen centerline was placed along the center of the seam weld in the longitudinal direction. This particular specimen geometry was intended to determine the CTOA of the weld metal. Although fatigue precracks were successfully placed at the weld centerline, during CTOA testing, the cracks inevitably diverted into the HAZs upon crack extension. Figure 13 shows an example of this where the crack propagated essentially vertically through the weld metal until it found the HAZ. The crack proceeded to follow the crack along the HAZ for the remainder of the test. Values for the CTOA of the HAZ from these specimens were similar to those obtained from the specimens made with the HAZ in the center of the test section, as shown in Table 4.

Figure 13A shows the entire post-test specimen in which the growing crack deviated into the HAZ. The nature of crack progression through the HAZ is illustrated in Fig. 14B, C, which shows the cross section of the fracture 10 and 40 mm from the end of the fatigue precrack, respectively. The orientation of the growing crack was remarkably consistent along the length of the CTOA specimen, as it followed a path parallel to the weld interface of the first pass.

Based on the hardness measurements collected from the side of the weld that did not fracture, the crack advanced through the high-temperature HAZ at the location where the hardness levels dropped to levels observed in the base metal. It is worth noting that the first and second passes of the weld deposits were not aligned on a common centerline, as they appear offset in Fig. 6A. This likely affected the crack extension in the following way. The crack diverted immediately from the weld metal at the beginning of the CTOA test since the weld metal had higher resistance to crack extension than the HAZ. Therefore, the crack moved into the HAZ, to the site of the weak link (the high-temperature HAZ from the first pass) where no weld metal from the second pass was in its path. Note that on the left side of the weld in Fig. 6A, there is a large amount of weld metal from the second pass between the surface and the high-temperature HAZ of the first pass. Since the right side of the weld metal had very little weld metal from the second pass in this region, it was the easier side for crack extension to occur. This is a significant result since weld alignment may affect where the crack will propagate in certain welded joints.

Discussion

Girth Weld

Girth weld metal is similar in strength to that of the base metal in this pipe, unlike what is typically achieved in joints in lower strength pipe. Nevertheless, it was observed that the values for CTOA obtained from the girth weld material were quite small.

The observed values for CTOA in the girth weld specimen were affected by interfaces and changes in material properties near the weld interface of the weld. The measured CTOA recorded in the HAZ is the result of composite behavior of the joint, and, therefore, does not reflect the HAZ material alone. As mentioned in the Metallography section, the softer girth weld HAZ is only 2 to 3 mm wide, which likely limits its influence on the local stress/strain field, but the weld interface poses an abrupt change in material properties that could permit stresses to concentrate at the interface and increase the measured CTOA. Although the HAZ was too narrow to accurately measure its ductile-fracture resistance, it is of interest that this test can show how a slow-growing crack might be influenced by the presence of a girth weld and predict what increases in load might be needed for continued crack extension through the weld.

The mechanisms that cause a change in the fracture orientation of a growing crack are not understood. It appears that the presence of the girth weld, however, can exert an influence as far as 10 mm away, as observed in Fig. 10. Furthermore, the growing crack was more than 7 mm away when the second crack started opening up within the weld. The girth weld, its associated interfaces, and residual stresses create a complex system that makes it difficult to isolate individual contributions to changes in values of CTOA.

Steady-state crack extension through the girth weld was not attained. Many contradictions to steady state were observed including: increases in CTOA, variable crack extension rates, changes in the slope of load vs. displacement, and deviation in crack path. Lastly, the plastic deformation ahead of the crack tip was distorted due to the presence of the fusion boundary and changes in microstructure. Although not steady state, the behavior associated with the crack extension is quantifiable for these test conditions and has the potential to be useful in the modeling of crack extension and growth in pipelines and their girth welds.

Seam Weld

The welding processes used for the seam weld (SAW) and the girth weld (SMAW) had significantly different heat inputs and so produced HAZs with different widths (8 vs. 3 mm), grain sizes (5.5 vs. 4.3 μm), and hardness (275 vs. 240 HV, depending on which region of the seam weld HAZ is being compared). The wide HAZ and orientation of the seam weld allowed measurement of the CTOA properties of the associated HAZ.

When testing the seam weld HAZ, the crack was oriented parallel to its length, unlike the girth weld specimen. The stress field above and below the crack may be constrained by the base material and the weld, but the crack was able to grow without crossing material interfaces, as occurred with the girth weld specimens. Comparisons between values of CTOA from the HAZ of the seam weld and the girth weld are not possible, for reasons stated previously. The mean value for CTOA from the seam-weld HAZ is ~7 deg. This value is less than the ~9-deg value for the X100 base metal (Ref. 10), showing that the seam-weld HAZ has comparatively low resistance to crack extension.

CTOA tests of the seam-weld metal were unsuccessful as the crack jumped out of the weld into a region of the HAZ with the lowest hardness. This suggests that since the HAZ is the weakest link in this material system, a crack running in an actual pipeline would also preferentially jump to the HAZ and propagate in that location. Therefore, the test result showed qualitatively the preferential location of failure. The current design of the MDCB specimen presented particular challenges for obtaining results from the seam weld. The weld is not wide enough so that the entire reduced section can comprise the weld. This permits the crack to deviate into the associated HAZ. Narrowing the reduced section or side-

grooving the specimen could help to maintain the crack in the weld. Further work needs to be conducted to explore these and other alternatives.

Hashemi et al. (Ref. 3) and Shterenlikht et al. (Ref. 5) tested MDCB specimens with gauge thicknesses of 8, 10, and 12 mm, and 4, 8, and 10 mm, respectively. Neither group found that the thickness influenced the value for CTOA. This led them to conclude that CTOA is a fracture parameter. In this work, however, the values for the CTOA from the girth weld and the seam-weld HAZ were significantly smaller for the 3-mm specimens than for the 8-mm specimens. Although not reported here, it was found that, similarly, base metal tests on 3- and 8-mm specimens also resulted in smaller CTOA values from the thinner specimens (Ref. 11). These results would imply that there is a threshold thickness below which the constraints change sufficiently to affect the CTOA. This issue merits further investigation.

Summary and Conclusions

The current work was performed to evaluate the use of the CTOA test for determining the resistance to ductile fracture of high-strength welded pipeline materials. A girth weld made with the SMAW process was tested with the crack running perpendicularly (transverse) to the weld. A seam weld made with the SAW process was tested with the cracking running parallel (longitudinal) to the weld. Variations in microstructure, hardness, and weld orientation influenced the CTOA, crack extension rates, and crack propagation paths. Based on this work, the following conclusions can be made:

- MDCB specimen thickness influenced measurement of CTOA values. In general, testing of 8-mm-thick specimens resulted in higher CTOA values than 3-mm-thick specimens. The relationship between plastic collapse and thickness is not fully understood from these tests.
- CTOA testing of girth welds was influenced by the composite nature of the weldment, which included geometrical changes at interfaces between various weld regions, and the presence of residual stresses. These issues prevented steady-state crack extension through the girth weld and complicated CTOA measurement.
- Girth weld tests of 8-mm-thick specimens revealed that CTOA values were highest in the HAZ (~11 deg), although these values were affected by the composite behavior of the weldment. The base metal had lower CTOA values (~9 deg) than the HAZ, followed by the weld metal (~7 deg).
- Crack paths across the girth weld were irregular in nature and propagation through the HAZ was immediate compared to the slower advance rates in other weld regions.
- During each of the four CTOA tests with the crack initiated in the seam weld metal, the cracks immediately sought the lowest energy path out of the weld metal after the onset of crack growth, and then propagated through the HAZ with lowest hardness. This precluded measurement of CTOA from the seam weld. Whether the issue was the weld having higher toughness or the HAZ having lower strength is not known with the data collected.
- The seam weld HAZ had a lower tearing resistance as compared with the base metal (~9 deg), with a CTOA of ~7 deg for the 8-mm-thick specimen.
- Fracture surfaces of CTOA specimens were typically slant or double slant and exhibited considerable microscopic ductility. Fracture was typically fully slant at the HAZ and weld metal after CTOA testing of girth welds.

Acknowledgments

The authors thank the U.S. Department of Transportation for financial support; J. Matthew Treinen, Ryan Johns, Marc Dvorak, and Ross Rentz of NIST for their assistance; and Jim Newman of Mississippi State University and Jim Fekete of NIST for their excellent reviews of the manuscript.

References

1. Horsley, D. J. 2003. Background to the use of CTOA for prediction of dynamic ductile fracture arrest in pipelines. *Eng. Fract.Mech.* 70, pp. 547–552.

2. Rudland, D. L., Wilkowski, G. M., Feng, Z., Wang, Y. –Y., Horsley, D., and Glover, A. 2003. Experimental investigation of CTOA in linepipe steels. *Eng. Fract. Mech.* 70, pp. 567–577.

3. Hashemi, S. H., Howard, I. C., Yates, J. R., Andrews, R. M., and Edwards, A. M. 2004. Experimental study of the thickness and fatigue precracking influence on the CTOA toughness values of high grade gas pipeline steel. *Proc. Int. Pipeline Conf.*, IPC04-0681.

4. Hashemi, S. H., Howard, I. C., Yates, J. R., Andrews, R. M., and Edwards, A. M. 2004. A single specimen CTOA test method for evaluating the crack tip opening angle in gas pipeline steels. *Proc. Int. Pipeline Conf.*, IPC04-0610.

5. Shterenlikht, A., Hashemi, S. H., Howard, I. C., Yates, J. R., and Andrews, R. M. 2004. A specimen for studying the resistance to ductile crack propagation in pipes. *Eng. Frac. Mech.* 71, pp. 1997–2013.

6. Darcis, P. P., McCowan, C. N., Windhoff, H., McColskey, J. D., and Siewert, T. A. 2008. Crack tip opening angle optical measurement methods in five pipeline steels. *Eng. Frac. Mech.* 75, pp. 2453–2468.

7. Liu, M., Wang, Y. –Y., and Horsley, D. 2005. Significance of HAZ softening on strain concentration and crack driving force in pipeline girth welds. *Proc. 24th Int. Conf. Offshore Mech. Arctic. Eng.*, pp. 385–393.

8. Hudson, M., Di Vito, L., Demofonti, G., Aristotile, R., Andrews, R., and Slater, S. 2004. X100 — Girth welding, joint properties and defect tolerance. Welding Engineering Research Center, Cranfield University, *www.msm.cam.ac.uk/phasetrans/2005/LINK/176.pdf*

9. Darcis, P. P, Kohn, G., Bussiba, A., McColskey, J. D., McCowan, C. N., Fields, R., Smith, R., and Merritt, J. 2006. Crack tip opening angle: Measurement and modeling of fracture resistance in low and high strength pipeline steels. *Proc. Int. Pipeline Conf.*, IPC2006-10172.

10. Reuven, R., Drexler, E., McCowan, C., Darcis, P., Treinen, M., Smith, R., Merritt, J., Siewert, T., and McColskey, D. 2008. CTOA results for X65 and X100 pipeline steels: Influence of displacement rate. *Proc. Int. Pipeline Conf.*, IPC2008-64363.

11. Darcis, Ph. P., Drexler, E. S., Fields, R., McColskey, J. D., McCowan, C. N., Reuven, R., and Siewert, T. A. 2009, Crack tip opening angle applications and developments in pipeline industry. *12th Intl. Conf Fract. 2009*, Paper T35.005.

Iron Man Comic Book, Welding Career DVDs Available for Free

Copies of four unique resource materials, including the *Careers In Welding* magazine, *Iron Man* comic book, and *Hot Bikes, Fast Cars, Cool Careers* and *Careers In Welding* DVDs, may be requested for free.

Just visit *www.CareersInWelding.com*, click on the welding publications link, and fill out the form specifying the quantity you need of each item.

Submit a New Products Item for Consideration

If your company has a new welding, fabricating, or manufacturing product readily available, the details required to be considered for possible publication in the *Welding Journal* are as follows:

• Press release with the product's name, important features, and specific industries it's aimed for

• High-resolution jpg or tiff photo (266 or more dpi).

Please e-mail submissions to Associate Editor Kristin Campbell at *kcampbell@aws.org*.